Updated determination of D 0 - D 0 mixing and C P violation parameters with D 0 → K + π -

Aaij, R.; Adeva, B.; Adinolfi, M.; Ajaltouni, Z.; Akar, S.; Albrecht, J.; Alessio, F.; Alexander, M.; Alfonso Albero, A.; Ali, S.; Alkhazov, G.; Alvarez Cartelle, P.; Alves, A. A.; Amato, S.; Amerio, S.; Amhis, Y.; An, L.; Anderlini, L.; Andreassi, G.; Andreotti, M.

DOI:
10.1103/PhysRevD.97.031101

Document Version
Publisher's PDF, also known as Version of record

Rapid Communications

Updated determination of D^0–$\bar{D}^0$ mixing and CP violation parameters with $D^0 \to K^+\pi^-$ decays

R. Aaij *et al.*[*]
(LHCb Collaboration)

(Received 8 December 2017; published 22 February 2018; corrected 26 March 2018)

We report measurements of charm-mixing parameters based on the decay-time-dependent ratio of $D^0 \to K^+\pi^-$ to $D^0 \to K^-\pi^+$ rates. The analysis uses a data sample of proton-proton collisions corresponding to an integrated luminosity of 5.0 fb^{-1} recorded by the LHCb experiment from 2011 through 2016. Assuming charge-parity (CP) symmetry, the mixing parameters are determined to be $x'^2 = (3.9 \pm 2.7) \times 10^{-5}$, $y' = (5.28 \pm 0.52) \times 10^{-3}$, and $R_D = (3.454 \pm 0.031) \times 10^{-3}$. Without this assumption, the measurement is performed separately for D^0 and $\bar{D}^0$ mesons, yielding a direct CP-violating asymmetry $A_D = (-0.1 \pm 9.1) \times 10^{-3}$, and magnitude of the ratio of mixing parameters $1.00 < |q/p| < 1.35$ at the 68.3% confidence level. All results include statistical and systematic uncertainties and improve significantly upon previous single-measurement determinations. No evidence for CP violation in charm mixing is observed.

DOI: 10.1103/PhysRevD.97.031101

I. INTRODUCTION

The mass eigenstates of neutral charm mesons are linear combinations of the flavor eigenstates, $|D_{1,2}\rangle = p|D^0\rangle \pm q|\bar{D}^0\rangle$, where p and q are complex-valued coefficients. This results in D^0–$\bar{D}^0$ oscillations. In the limit of charge-parity (CP) symmetry, oscillations are characterized by the dimensionless differences in mass, $x \equiv \Delta m/\Gamma \equiv (m_2 - m_1)/\Gamma$, and decay width, $y \equiv \Delta\Gamma/2\Gamma \equiv (\Gamma_2 - \Gamma_1)/2\Gamma$, between the CP-even (D_2) and CP-odd (D_1) mass eigenstates, where Γ is the average decay width of neutral D mesons. If CP symmetry does not hold, the oscillation probabilities for mesons produced as D^0 and $\bar{D}^0$ can differ, further enriching the phenomenology. Long- and short-distance amplitudes govern the oscillations of neutral D mesons [1–3]. Long-distance amplitudes depend on the exchange of low-energy gluons and are challenging to calculate. Short-distance amplitudes may include contributions from a broad class of particles not described in the standard model, which might affect the oscillation rate or introduce a difference between the D^0 and $\bar{D}^0$ meson decay rates. The study of CP violation in D^0 oscillations therefore offers sensitivity to non-standard-model phenomena [4–7].

The first evidence for D^0–$\bar{D}^0$ oscillations was reported in 2007 [8,9]. More recently, precise results from the LHCb Collaboration [10–15] improved the knowledge of the mixing parameters, $x = (4.6^{+1.4}_{-1.5}) \times 10^{-3}$ and $y = (6.2 \pm 0.8) \times 10^{-3}$ [16], although neither a nonzero value for the mass difference nor a departure from CP symmetry have been established.

This paper reports measurements of CP-averaged and CP-violating mixing parameters in D^0–$\bar{D}^0$ oscillations based on the comparison of the decay-time-dependent ratio of $D^0 \to K^+\pi^-$ to $D^0 \to K^-\pi^+$ rates with the corresponding ratio for the charge-conjugate processes. The analysis uses data corresponding to an integrated luminosity of 5.0 fb^{-1} from proton-proton (pp) collisions at 7, 8, and 13 TeV center-of-mass energies, recorded with the LHCb experiment from 2011 through 2016. This analysis improves upon a previous measurement [12], owing to the tripling of the sample size and an improved treatment of systematic uncertainties. The inclusion of charge-conjugate processes is implicitly assumed unless stated otherwise.

The neutral D-meson flavor at production is determined from the charge of the low-momentum pion (soft pion), π_s^+, produced in the flavor-conserving strong-interaction decay $D^*(2010)^+ \to D^0\pi_s^+$. The shorthand notation D^{*+} is used to indicate the $D^*(2010)^+$ meson throughout. We denote as right-sign (RS) the $D^{*+} \to D^0(\to K^-\pi^+)\pi_s^+$ process, which is dominated by a Cabibbo-favored amplitude. Wrong-sign (WS) decays, $D^{*+} \to D^0(\to K^+\pi^-)\pi_s^+$, arise from the doubly Cabibbo-suppressed $D^0 \to K^+\pi^-$ decay and the Cabibbo-favored $\bar{D}^0 \to K^+\pi^-$ decay that follows D^0–$\bar{D}^0$ oscillation. Since the mixing parameters are small, $|x|, |y| \ll 1$, the CP-averaged decay-time-dependent ratio of WS-to-RS rates is approximated as [1–4]

$$R(t) \approx R_D + \sqrt{R_D}y'\frac{t}{\tau} + \frac{x'^2 + y'^2}{4}\left(\frac{t}{\tau}\right)^2, \qquad (1)$$

[*]Full author list given at the end of the article.

where t is the proper decay time, τ is the average D^0 lifetime, and R_D is the ratio of suppressed-to-favored decay rates. The parameters x' and y' depend on the mixing parameters, $x' \equiv x\cos\delta + y\sin\delta$ and $y' \equiv y\cos\delta - x\sin\delta$, through the strong-phase difference δ between the suppressed and favored amplitudes, $\mathcal{A}(D^0 \to K^+\pi^-)/\mathcal{A}(\bar{D}^0 \to K^+\pi^-) = -\sqrt{R_D}e^{-i\delta}$, which was measured at the CLEO-c and BESIII experiments [17,18]. If CP violation occurs, the decay-rate ratios $R^+(t)$ and $R^-(t)$ of mesons produced as D^0 and $\bar{D}^0$, respectively, are functions of independent sets of mixing parameters, $R_D^{\pm}$, $(x'^{\pm})^2$, and $y'^{\pm}$. The parameters R_D^+ and R_D^- differ if the ratio between the suppressed and favored decay amplitudes is not CP symmetric, indicating direct CP violation. Violation of CP symmetry either in mixing, $|q/p| \neq 1$, or in the interference between mixing and decay amplitudes, $\phi \equiv \arg[q\mathcal{A}(\bar{D}^0 \to K^+\pi^-)/p\mathcal{A}(D^0 \to K^+\pi^-)] \neq \delta$, are referred to as manifestations of indirect CP violation and generate differences between $((x'^+)^2, y'^+)$ and $((x'^-)^2, y'^-)$.

Experimental effects such as differing efficiencies for reconstructing WS and RS decays may bias the observed ratios of signal decays and, therefore, the mixing-parameter results. We assume that the efficiency for reconstructing and selecting the $K^{\mp}\pi^{\pm}\pi_s^+$ final state approximates as the product of the efficiency for the $K^{\mp}\pi^{\pm}$ pair from the D^0 decay and the efficiency for the soft pion. The observed WS-to-RS yield ratio then equals $R(t)$ multiplied by the ratio of the efficiencies for reconstructing $K^+\pi^-$ and $K^-\pi^+$ pairs, which is the only relevant instrumental nuisance. The asymmetry in production rates between D^{*+} and D^{*-} mesons in the LHCb acceptance and asymmetries in detecting soft pions of different charges cancel in the WS-to-RS ratio.

Candidate D^{*+} mesons produced directly in the collision (primary D^{*+}) are reconstructed while suppressing background contributions from charm mesons produced in the decay of bottom hadrons (secondary D^{*+}) and misreconstructed decays. Residual contaminations from such backgrounds are measured using control regions. The asymmetry in $K^{\pm}\pi^{\mp}$ reconstruction efficiency is estimated using control samples of charged D-meson decays. The yields of RS and WS primary D^{*+} candidates are determined, separately for each flavor, in intervals (bins) of decay time by fitting the D^{*+} mass distribution of candidates consistent with being D^0 decays. We fit the resulting WS-to-RS yield ratios as a function of decay time to measure the mixing and CP-violation parameters, including the effects of instrumental asymmetries, residual background contamination, and all considered systematic contributions. To ensure unbiased results, the differences in the decay-time dependence of the WS D^0 and $\bar{D}^0$ samples are not examined until the analysis procedure is finalized.

II. THE LHCB DETECTOR

The LHCb detector [19] is a single-arm forward spectrometer covering the pseudorapidity range $2 < \eta < 5$, designed for the study of particles containing b or c quarks. The detector achieves high precision charged-particle tracking using a silicon-strip vertex detector surrounding the pp interaction region, a large-area silicon-strip detector located upstream of a dipole magnet with a bending power of about 4 Tm, and three layers of silicon-strip detectors and straw drift tubes placed downstream of the magnet. The tracking system provides a measurement of charged-particle momentum p with a relative uncertainty varying from 0.5% at low momentum to 1.0% at 200 GeV/c. The typical decay-time resolution for $D^0 \to K^+\pi^-$ decays is 10% of the D^0 lifetime. The polarity of the dipole magnet is reversed periodically throughout data-taking. The minimum distance of a charged-particle trajectory (track) to a proton-proton interaction space-point (primary vertex), the impact parameter, is measured with $(15 + 29/p_T)$ μm resolution, where p_T is the component of the momentum transverse to the beam, in GeV/c. Charged hadrons are identified using two ring-imaging Cherenkov detectors. Photons, electrons, and hadrons are identified by scintillating-pad and preshower detectors, and an electromagnetic and a hadronic calorimeter. Muons are identified by alternating layers of iron and multiwire proportional chambers. The online event selection is performed by a hardware trigger, based on information from the calorimeter and muon detectors, followed by a software trigger, based on information on displaced charged particles reconstructed in the event. Offline-like quality detector alignment and calibrations, performed between the hardware and software stages, are available to the software trigger for the 2015 and 2016 data [20,21]. Hence, for these data the analysis uses candidates reconstructed in the software trigger to reduce event size.

III. EVENT SELECTION AND CANDIDATE RECONSTRUCTION

Events enriched in D^{*+} candidates originating from the primary vertex are selected by the hardware trigger by imposing that either one or more D^0 decay products are consistent with depositing a large transverse energy in the calorimeter or that an accept decision is taken independently of the D^0 decay products and soft pion. In the software trigger, one or more D^0 decay products are required to be inconsistent with charged particles originating from the primary vertex and, for 2015 and 2016 data, loose particle-identification criteria are imposed on these final-state particles. Each D^0 candidate is then combined with a low-momentum positive-charge particle originating from the primary vertex to form a D^{*+} candidate.

In the offline analysis, criteria on track and primary-vertex quality are imposed. To suppress the contamination from misidentified two-body D^0 decays, the pion and kaon candidates from the D^0 decay are subjected to stringent particle-identification criteria. An especially harmful background is generated by a 3% contribution of soft pions misreconstructed by combining their track segments in the

vertex detector with unrelated segments in the downstream tracking detectors. The track segments in the vertex detector are genuine, resulting in properly measured opening angles in the $D^{*+} \to D^0\pi_s^+$ decay. Since the opening angle dominates over the π_s^+ momentum in the determination of the D^{*+} mass, such spurious soft pions tend to produce a signal-like peak in the D^{*+} mass spectrum. In addition, they bias the WS-to-RS ratio because the mistaken association with downstream track segments is prone to charge mismeasurements. We suppress such candidates with stringent requirements on a dedicated discriminant based on many low-level variables associated with track reconstruction [22]. Candidates consistent with the D^{*+} decay topology are reconstructed by computing the two-body mass $M(D^0\pi_s^+)$ using the known D^0 and π^+ masses [23] and the reconstructed momenta [24]. The mass resolution is improved by nearly a factor of 2 with a kinematic fit that constrains the D^{*+} candidate to originate from a primary vertex [25]. If multiple primary vertices are reconstructed, the vertex resulting from the fit with the best χ^2 probability is chosen. The sample is further enriched in primary charm decays by restricting the impact-parameter chi-squared, $\chi^2_{\rm IP}$, of the D^0 and π_s^+ candidates such that the candidates point to the primary vertex. The $\chi^2_{\rm IP}$ variable is the difference between the χ^2 of the primary-vertex fit reconstructed including or excluding the considered particle, and offers a measure of consistency with the hypothesis that the particle originates from the primary vertex. Only opposite-charge particle pairs with $K^{\mp}\pi^{\pm}$ mass within 24 MeV/c^2 (equivalent to approximately three times the mass resolution) of the known D^0 mass [23] and K^+K^- and $\pi^+\pi^-$ masses more than 40 MeV/c^2 away from the D^0 mass are retained. Accidental combinations of a genuine D^0 with a random soft pion are first suppressed by removing the 13% of events where more than one D^{*+} candidate is reconstructed. We then use an artificial neural-network discriminant that exploits the π_s^+ pseudorapidity, transverse momentum, and particle-identification information, along with the track multiplicity of the event. The discriminant is trained on an independent RS sample to represent the WS signal features and on WS events containing multiple candidates to represent background. Finally, we remove from the WS sample events where the same D^0 candidate is also used to reconstruct a RS decay, which reduces the background by 16% with no significant loss of signal.

IV. YIELD DETERMINATION

The RS and WS signal yields are determined by fitting the $M(D^0\pi_s^+)$ distribution of D^0 signal candidates. The decay-time-integrated $M(D^0\pi_s^+)$ distributions of the selected RS and WS candidates are shown in Fig. 1. The smooth background is dominated by favored $D^0 \to K^-\pi^+$ and $\bar{D}^0 \to K^+\pi^-$ decays associated with random soft-pion candidates. The sample contains approximately 1.77×10^8 RS and 7.22×10^5 WS signal decays. Each sample is divided into 13 subsamples according to the decay time, and signal yields are determined for each subsample using an empirical shape [11]. We assume that the signal shapes are common to WS and RS decays for a given D^* meson flavor whereas the descriptions of the backgrounds are independent. The decay-time-dependent WS-to-RS rate ratios R^+ and R^- observed in the D^0 and $\bar{D}^0$ samples, respectively, and their difference, are shown in Fig. 2. The ratios and difference include corrections for the relative efficiencies for reconstructing $K^-\pi^+$ and $K^+\pi^-$ final states.

V. DETERMINATION OF OSCILLATION PARAMETERS

The mixing parameters are determined by minimizing a χ^2 function that includes terms for the difference between

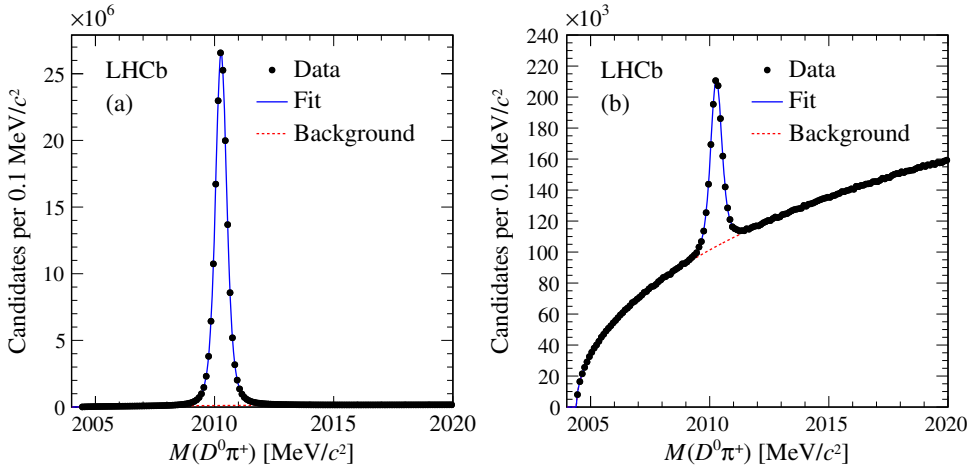

FIG. 1. Distribution of $M(D^0\pi_s^+)$ for selected (a) right-sign $D^0 \to K^-\pi^+$ and (b) wrong-sign $D^0 \to K^+\pi^-$ candidates.

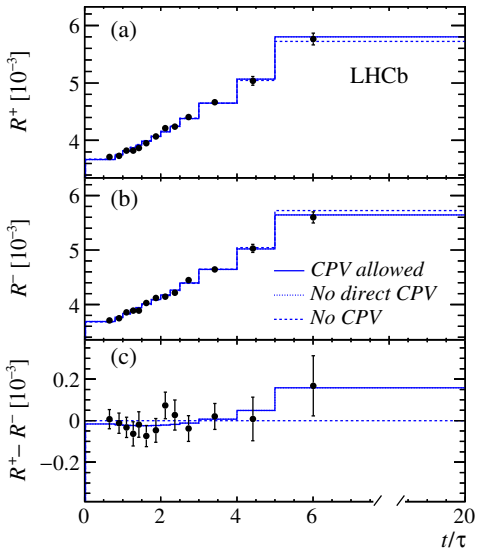

FIG. 2. Efficiency-corrected ratios of WS-to-RS yields for (a) D^{*+} decays, (b) D^{*-} decays, and (c) their differences as functions of decay time in units of D^0 lifetime. Projections of fits allowing for (dashed line) no CP violation, (dotted line) no direct CP violation, and (solid line) direct and indirect CP violation are overlaid. The last two curves overlap. The abscissa of each data point corresponds to the average decay time over the bin. The error bars indicate the statistical uncertainties.

the observed and predicted ratios and for systematic effects,

$$\chi^2 = \sum_i \left[\left(\frac{r_i^+ - \epsilon_r^+ \tilde{R}_i^+}{\sigma_i^+} \right)^2 + \left(\frac{r_i^- - \epsilon_r^- \tilde{R}_i^-}{\sigma_i^-} \right)^2 \right] + \chi^2_{\text{corr}}. \quad (2)$$

The observed WS-to-RS yield ratio and its statistical uncertainty in the decay-time bin i are denoted by $r_i^\pm$ and $\sigma_i^\pm$, respectively. The associated predicted value $\tilde{R}_i^\pm$ corresponds to the decay-time integral over bin i of Eq. (1), including bin-specific corrections. The parameters associated with these corrections are determined separately for data collected in different LHC and detector configurations and vary independently in the fit within their constraint χ^2_{corr} in Eq. (2). Such corrections account for small biases due to (i) the decay-time evolution of the 1%–10% fraction of signal candidates originating from b-hadron decays, (ii) the approximately 0.3% component of the background from misreconstructed charm decays that peak in the signal region, and (iii) the effect of instrumental asymmetries in the $K^\pm\pi^\mp$ reconstruction efficiencies. The secondary-D^{*+} fraction is determined by fitting, in each decay-time bin, the χ^2_{IP} distribution of RS D^0 signal decays. The peaking background, dominated by $D^0 \to K^-\pi^+$ decays in which both final-state particles are misidentified, is determined by extrapolating into the D^0 signal mass region the contributions from misreconstructed charm decays identified by reconstructing the two-body mass under various mass hypotheses for the decay products. The relative efficiency $\epsilon_r^\pm$ accounts for the effects of instrumental asymmetries in the $K^\pm\pi^\mp$ reconstruction efficiencies, mainly caused by K^- mesons having a larger nuclear interaction cross section with matter than K^+ mesons. These asymmetries are measured in data to be typically 0.01 with 0.001 precision, independent of decay time. They are derived from the efficiency ratio $\epsilon_r^+ = 1/\epsilon_r^- = \epsilon(K^+\pi^-)/\epsilon(K^-\pi^+)$, obtained by comparing the ratio of $D^- \to K^+\pi^-\pi^-$ and $D^- \to K^0_S(\to \pi^+\pi^-)\pi^-$ yields with the ratio of the corresponding charge-conjugate decay yields. The asymmetry between D^+ and D^- production rates [26] cancels in this ratio, provided that the kinematic distributions are consistent across samples. We therefore weight the $D^- \to K^+\pi^-\pi^-$ candidates so that their kinematic distributions match those in the $D^- \to K^0_S\pi^-$ sample. We then determine $\epsilon_r^\pm$ as functions of kaon momentum to account for the known momentum dependence of the asymmetry between K^+ and K^- interaction rates with matter. In addition, a systematic uncertainty for possible residual contamination from spurious soft pions is included through a 1.05–1.35 scaling of the overall uncertainties. The scaling value is chosen such that a fit with a constant function of the time-integrated WS-to-RS ratio versus false-pion probability has unit reduced χ^2.

The observed WS-to-RS yield ratios for the D^0 and $\bar{D}^0$ samples are studied first with bin-by-bin arbitrary offsets designed to mimic the effect of significantly different mixing parameters in the two samples. To search for residual systematic uncertainties, the analysis is repeated on statistically independent data subsets chosen according to criteria likely to reveal biases from specific instrumental effects. These criteria include the data-taking year (2011–2012 or 2015–2016), the magnet field orientation, the number of primary vertices in the event, the candidate multiplicity per event, the trigger category, the D^0 momentum and χ^2_{IP} with respect to the primary vertex, and the per-candidate probability to reconstruct a spurious soft pion. The resulting variations of the measured CP-averaged and CP-violating parameters are consistent with statistical fluctuations, with p values distributed uniformly in the 4%–85% range.

VI. RESULTS

The efficiency-corrected WS-to-RS yield ratios are subjected to three fits. The first fit allows for direct and indirect CP violation; the second allows only for indirect CP violation by imposing $R_D^+ = R_D^-$; and the third is a fit under the CP-conservation hypothesis, in which all mixing parameters are common to the D^0 and $\bar{D}^0$ samples. The fit results and their projections are presented in Table I and Fig. 2, respectively. Figure 3 shows the central values and confidence regions in the (x'^2, y') plane. For each fit, 208 WS-to-RS ratio data points are used, corresponding to 13 ranges of decay time, distinguishing D^{*+} from D^{*-} decays, two magnetic-field orientations, and 2011, 2012, 2015,

TABLE I. Results of fits for different CP-violation hypotheses. The first contribution to the uncertainties is statistical and the second systematic. Correlations include both statistical and systematic contributions.

	Results $[10^{-3}]$						
		Direct and indirect CP violation			Correlations		
Parameter	Value	R_D^+	y'^+	$(x'^+)^2$	R_D^-	y'^-	$(x'^-)^2$
R_D^+	$3.454 \pm 0.040 \pm 0.020$	1.000	−0.935	0.843	−0.012	−0.003	0.002
y'^+	$5.01 \pm 0.64 \pm 0.38$		1.000	−0.963	−0.003	0.004	−0.003
$(x'^+)^2$	$0.061 \pm 0.032 \pm 0.019$			1.000	0.002	−0.003	0.003
R_D^-	$3.454 \pm 0.040 \pm 0.020$				1.000	−0.935	0.846
y'^-	$5.54 \pm 0.64 \pm 0.38$					1.000	−0.964
$(x'^-)^2$	$0.016 \pm 0.033 \pm 0.020$						1.000
		No direct CP violation					
Parameter	Value	R_D	y'^+	$(x'^+)^2$	y'^-	$(x'^-)^2$	
R_D	$3.454 \pm 0.028 \pm 0.014$	1.000	−0.883	0.745	−0.883	0.749	
y'^+	$5.01 \pm 0.48 \pm 0.29$		1.000	−0.944	0.758	−0.644	
$(x'^+)^2$	$0.061 \pm 0.026 \pm 0.016$			1.000	−0.642	0.545	
y'^-	$5.54 \pm 0.48 \pm 0.29$				1.000	−0.946	
$(x'^-)^2$	$0.016 \pm 0.026 \pm 0.016$					1.000	
		No CP violation					
Parameter	Value	R_D	y'	x'^2			
R_D	$3.454 \pm 0.028 \pm 0.014$	1.000	−0.942	0.850			
y'	$5.28 \pm 0.45 \pm 0.27$		1.000	−0.963			
x'^2	$0.039 \pm 0.023 \pm 0.014$			1.000			

and 2016 data sets. The consistency of the data with the hypothesis of CP symmetry is determined from the change in χ^2 probability between the fit that assumes CP conservation and the fit in which CP violation is allowed. The resulting p value is 0.57 (0.37) for the fit in which both direct and indirect (indirect only) CP violation is allowed, showing that the data are compatible with CP symmetry.

The fit uncertainties incorporate both statistical and systematic contributions. The statistical uncertainty, determined in a separate fit by fixing all nuisance parameters to their central values, dominates the total uncertainty. The systematic component is obtained by subtraction in quadrature. The leading systematic uncertainty is due to residual secondary-D^{*+} contamination and does not exceed half of the statistical uncertainty. The second largest contribution is due to spurious soft pions. Smaller effects are due to peaking backgrounds for the CP-averaged results and uncertainties in detector asymmetries for the CP-violating results. All reported results, p values, and the contours shown in Fig. 3, include total uncertainties.

Direct CP violation would produce a nonzero intercept at $t = 0$ in the efficiency-corrected difference of WS-to-RS

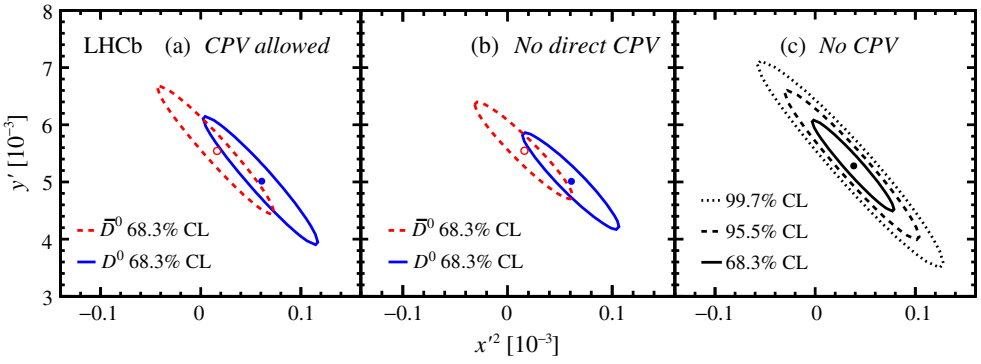

FIG. 3. Two-dimensional confidence regions in the (x'^2, y') plane obtained (a) without any restriction on CP violation, (b) assuming no direct CP violation, and (c) assuming CP conservation. The dashed (solid) curves in (a) and (b) indicate the contours of the mixing parameters associated with $\bar{D}^0$ (D^0) decays. The best-fit value for $\bar{D}^0$ (D^0) decays is shown with an open (filled) point. The solid, dashed, and dotted curves in (c) indicate the contours of CP-averaged mixing parameters at 68.3%, 95.5%, and 99.7% confidence levels (C.L.), respectively, and the point indicates the best-fit value.

yield ratios between D^0 and $\bar{D}^0$ mesons shown in Fig. 2(c). We parametrize this effect with the asymmetry measured in the fit that allows for direct CP violation, $A_D \equiv (R_D^+ - R_D^-)/(R_D^+ + R_D^-) = (-0.1 \pm 8.1 \pm 4.2) \times 10^{-3}$, where the first uncertainty is statistical and the second systematic. Indirect CP violation would result in a time dependence of the efficiency-corrected difference of yield ratios, which is not observed in Fig. 2(c). From the results of the fit allowing for direct and indirect CP violation, a likelihood for $|q/p|$ is constructed using the relations $x'^{\pm} = |q/p|^{\pm 1} \times (x' \cos\phi \pm y' \sin\phi)$ and $y'^{\pm} = |q/p|^{\pm 1}(y' \cos\phi \mp x' \sin\phi)$. Confidence intervals are derived with a likelihood-ratio ordering [27], assuming that the parameter correlations are independent of the true values of the mixing parameters. We determine $1.00 < |q/p| < 1.35$ and $0.82 < |q/p| < 1.45$ at the 68.3% and 95.5% confidence levels, respectively.

The R_D result departs from the previous result based on a subset of the same data [12], which was biased by the then-undetected residual spurious-pion background. Since such background induces an apparent global shift toward higher WS-to-RS ratio values, the bias affects predominantly the R_D measurement and less severely the mixing-parameter determination. The systematic uncertainties are significantly reduced because the dominant components are statistical in nature or sensitive to a generally improved understanding of the data quality.

VII. SUMMARY

We study D^0–$\bar{D}^0$ oscillations using $D^{*+} \to D^0(\to K^+\pi^-)\pi^+$ decays reconstructed in a data sample of pp collisions collected by the LHCb experiment from 2011 through 2016, corresponding to an integrated luminosity of 5.0 fb^{-1}. Assuming CP conservation, the mixing parameters are measured to be $x'^2 = (3.9 \pm 2.7) \times 10^{-5}$, $y' = (5.28 \pm 0.52) \times 10^{-3}$, and $R_D = (3.454 \pm 0.031) \times 10^{-3}$. The results are twice as precise as previous LHCb results [12] that were based on a subset of the present data, and supersede them. Studying D^0 and $\bar{D}^0$ decays separately shows no evidence for CP violation and provides the current most stringent bounds on the parameters A_D and $|q/p|$ from a single measurement, $A_D = (-0.1 \pm 9.1) \times 10^{-3}$ and $1.00 < |q/p| < 1.35$ at the 68.3% confidence level.

ACKNOWLEDGMENTS

We express our gratitude to our colleagues in the CERN accelerator departments for the excellent performance of the LHC. We thank the technical and administrative staff at the LHCb institutes. We acknowledge support from CERN and from the national agencies: CAPES, CNPq, FAPERJ and FINEP (Brazil); MOST and NSFC (China); CNRS/IN2P3 (France); BMBF, DFG and MPG (Germany); INFN (Italy); NWO (Netherlands); MNiSW and NCN (Poland); MEN/IFA (Romania); MinES and FASO (Russia); MinECo (Spain); SNSF and SER (Switzerland); NASU (Ukraine); STFC (United Kingdom); NSF (USA). We acknowledge the computing resources that are provided by CERN, IN2P3 (France), KIT and DESY (Germany), INFN (Italy), SURF (Netherlands), PIC (Spain), GridPP (United Kingdom), RRCKI and Yandex LLC (Russia), CSCS (Switzerland), IFIN-HH (Romania), CBPF (Brazil), PL-GRID (Poland) and OSC (USA). We are indebted to the communities behind the multiple open-source software packages on which we depend. Individual groups or members have received support from Alexander von Humboldt AvH Foundation (Germany), EPLANET, Marie Skłodowska-Curie Actions and ERC (European Union), ANR, Labex P2IO, ENIGMASS and OCEVU, and Région Auvergne-Rhône-Alpes (France), RFBR and Yandex LLC (Russia), GVA, XuntaGal and GENCAT (Spain), Herchel Smith Fund, the Royal Society, the English-Speaking Union and the Leverhulme Trust (United Kingdom).

[1] S. Bianco, F. L. Fabbri, D. Benson, and I. Bigi, A Cicerone for the physics of charm, Riv. Nuovo Cimento **26N7**, 1 (2003).
[2] G. Burdman and I. Shipsey, D^0–$\bar{D}^0$ mixing and rare charm decays, Annu. Rev. Nucl. Part. Sci. **53**, 431 (2003).
[3] M. Artuso, B. Meadows, and A. A. Petrov, Charm meson decays, Annu. Rev. Nucl. Part. Sci. **58**, 249 (2008).
[4] G. Blaylock, A. Seiden, and Y. Nir, The role of CP violation in D^0–$\bar{D}^0$ mixing, Phys. Lett. B **355**, 555 (1995).
[5] A. A. Petrov, Charm mixing in the standard model and beyond, Int. J. Mod. Phys. A **21**, 5686 (2006).
[6] E. Golowich, J. Hewett, S. Pakvasa, and A. A. Petrov, Implications of D^0–$\bar{D}^0$ mixing for new physics, Phys. Rev. D **76**, 095009 (2007).
[7] M. Ciuchini, E. Franco, D. Guadagnoli, V. Lubicz, M. Pierini, V. Porretti, and L. Silvestrini, D^0–$\bar{D}^0$ mixing and new physics: General considerations and constraints on the MSSM, Phys. Lett. B **655**, 162 (2007).
[8] B. Aubert *et al.* (BABAR Collaboration), Evidence for D^0–$\bar{D}^0$ Mixing, Phys. Rev. Lett. **98**, 211802 (2007).
[9] M. Staric *et al.* (Belle Collaboration), Evidence for D^0–$\bar{D}^0$ Mixing, Phys. Rev. Lett. **98**, 211803 (2007).

[10] R. Aaij *et al.* (LHCb Collaboration), Measurement of mixing and *CP* violation parameters in two-body charm decays, J. High Energy Phys. 04 (2012) 129.
[11] R. Aaij *et al.* (LHCb Collaboration), Observation of D^0–$\bar{D}^0$ Oscillations, Phys. Rev. Lett. **110**, 101802 (2013).
[12] R. Aaij *et al.* (LHCb Collaboration), Measurement of D^0–$\bar{D}^0$ Mixing Parameters and Search for *CP* Violation Using $D^0 \to K^+\pi^-$ Decays, Phys. Rev. Lett. **111**, 251801 (2013).
[13] R. Aaij *et al.* (LHCb Collaboration), Model-independent measurement of mixing parameters in $D^0 \to K^0_S\pi^+\pi^-$ decays, J. High Energy Phys. 04 (2016) 033.
[14] R. Aaij *et al.* (LHCb Collaboration), First observation of D^0–$\bar{D}^0$ oscillations in $D^0 \to K^+\pi^-\pi^+\pi^-$ decays and measurement of the associated coherence parameters, Phys. Rev. Lett. **116**, 241801 (2016).
[15] R. Aaij *et al.* (LHCb Collaboration), Measurements of charm mixing and *CP* violation using $D^0 \to K^\pm\pi^\mp$ decays, Phys. Rev. D **95**, 052004 (2017).
[16] Y. Amhis *et al.* (Heavy Flavor Averaging Group), Averages of *b*-hadron, *c*-hadron, and τ-lepton properties as of summer 2016, Eur. Phys. J. C **77**, 895 (2017), updated results and plots available at http://www.slac.stanford.edu/xorg/hflav/.
[17] D. M. Asner *et al.* (CLEO Collaboration), Updated measurement of the strong phase in $D^0 \to K^+\pi^-$ decay using quantum correlations in $e^+e^- \to D^0\bar{D}^0$ at CLEO, Phys. Rev. D **86**, 112001 (2012).
[18] M. Ablikim *et al.* (BESIII Collaboration), Measurement of the $D \to K^-\pi^+$ strong phase difference in $\psi(3770) \to D^0\bar{D}^0$, Phys. Lett. B **734**, 227 (2014).
[19] A. A. Alves, Jr. *et al.* (LHCb Collaboration), The LHCb detector at the LHC, J. Instrum. **3**, S08005 (2008).
[20] G. Dujany and B. Storaci, Real-time alignment and calibration of the LHCb Detector in Run II, J. Phys. Conf. Ser. **664**, 082010 (2015).
[21] R. Aaij *et al.*, Tesla: An application for real-time data analysis in high energy physics, Comput. Phys. Commun. **208**, 35 (2016).
[22] M. De Cian, S. Farry, P. Seyfert, and S. Stahl, Report No. LHCb-PUB-2017-011, https://cds.cern.ch/record/2255039?ln=en.
[23] C. Patrignani *et al.* (Particle Data Group), Review of particle physics, Chin. Phys. C **40**, 100001 (2016), and 2017 online update.
[24] T. Aaltonen *et al.* (CDF Collaboration), Measurement of *CP*–violating asymmetries in $D^0 \to \pi^+\pi^-$ and $D^0 \to K^+K^-$ decays at CDF, Phys. Rev. D **85**, 012009 (2012).
[25] W. D. Hulsbergen, Decay chain fitting with a Kalman filter, Nucl. Instrum. Methods Phys. Res., Sect. A **552**, 566 (2005).
[26] R. Aaij *et al.* (LHCb Collaboration), Measurement of the $D^\pm$ production asymmetry in 7 TeV pp collisions, Phys. Lett. B **718**, 902 (2013).
[27] G. J. Feldman and R. D. Cousins, A unified approach to the classical statistical analysis of small signals, Phys. Rev. D **57**, 3873 (1998).

Correction: The copyright statement contained an error and has been corrected.

R. Aaij,[40] B. Adeva,[39] M. Adinolfi,[48] Z. Ajaltouni,[5] S. Akar,[59] J. Albrecht,[10] F. Alessio,[40] M. Alexander,[53] A. Alfonso Albero,[38] S. Ali,[43] G. Alkhazov,[31] P. Alvarez Cartelle,[55] A. A. Alves Jr.,[59] S. Amato,[2] S. Amerio,[23] Y. Amhis,[7] L. An,[3] L. Anderlini,[18] G. Andreassi,[41] M. Andreotti,[17,a] J. E. Andrews,[60] R. B. Appleby,[56] F. Archilli,[43] P. d'Argent,[12] J. Arnau Romeu,[6] A. Artamonov,[37] M. Artuso,[61] E. Aslanides,[6] M. Atzeni,[42] G. Auriemma,[26] M. Baalouch,[5] I. Babuschkin,[56] S. Bachmann,[12] J. J. Back,[50] A. Badalov,[38,b] C. Baesso,[62] S. Baker,[55] V. Balagura,[7,c] W. Baldini,[17] A. Baranov,[35] R. J. Barlow,[56] C. Barschel,[40] S. Barsuk,[7] W. Barter,[56] F. Baryshnikov,[32] V. Batozskaya,[29] V. Battista,[41] A. Bay,[41] L. Beaucourt,[4] J. Beddow,[53] F. Bedeschi,[24] I. Bediaga,[1] A. Beiter,[61] L. J. Bel,[43] N. Beliy,[63] V. Bellee,[41] N. Belloli,[21,d] K. Belous,[37] I. Belyaev,[32,40] E. Ben-Haim,[8] G. Bencivenni,[19] S. Benson,[43] S. Beranek,[9] A. Berezhnoy,[33] R. Bernet,[42] D. Berninghoff,[12] E. Bertholet,[8] A. Bertolin,[23] C. Betancourt,[42] F. Betti,[15] M. O. Bettler,[40] M. van Beuzekom,[43] Ia. Bezshyiko,[42] S. Bifani,[47] P. Billoir,[8] A. Birnkraut,[10] A. Bizzeti,[18,e] M. Bjørn,[57] T. Blake,[50] F. Blanc,[41] S. Blusk,[61] V. Bocci,[26] T. Boettcher,[58] A. Bondar,[36,f] N. Bondar,[31] I. Bordyuzhin,[32] S. Borghi,[56,40] M. Borisyak,[35] M. Borsato,[39] F. Bossu,[7] M. Boubdir,[9] T. J. V. Bowcock,[54] E. Bowen,[42] C. Bozzi,[17,40] S. Braun,[12] J. Brodzicka,[27] D. Brundu,[16] E. Buchanan,[48] C. Burr,[56] A. Bursche,[16,g] J. Buytaert,[40] W. Byczynski,[40] S. Cadeddu,[16] H. Cai,[64] R. Calabrese,[17,a] R. Calladine,[47] M. Calvi,[21,d] M. Calvo Gomez,[38,b] A. Camboni,[38,b] P. Campana,[19] D. H. Campora Perez,[40] L. Capriotti,[56] A. Carbone,[15,h] G. Carboni,[25,i] R. Cardinale,[20,j] A. Cardini,[16] P. Carniti,[21,d] L. Carson,[52] K. Carvalho Akiba,[2] G. Casse,[54] L. Cassina,[21] M. Cattaneo,[40] G. Cavallero,[20,40,j] R. Cenci,[24,k] D. Chamont,[7] M. G. Chapman,[48] M. Charles,[8] Ph. Charpentier,[40] G. Chatzikonstantinidis,[47] M. Chefdeville,[4] S. Chen,[16] S. F. Cheung,[57] S.-G. Chitic,[40] V. Chobanova,[39] M. Chrzaszcz,[42] A. Chubykin,[31] P. Ciambrone,[19] X. Cid Vidal,[39] G. Ciezarek,[40] P. E. L. Clarke,[52] M. Clemencic,[40] H. V. Cliff,[49] J. Closier,[40] V. Coco,[40] J. Cogan,[6] E. Cogneras,[5] V. Cogoni,[16,g] L. Cojocariu,[30] P. Collins,[40] T. Colombo,[40] A. Comerma-Montells,[12] A. Contu,[16] G. Coombs,[40] S. Coquereau,[38] G. Corti,[40] M. Corvo,[17,a] C. M. Costa Sobral,[50]

B. Couturier,[40] G. A. Cowan,[52] D. C. Craik,[58] A. Crocombe,[50] M. Cruz Torres,[1] R. Currie,[52] C. D'Ambrosio,[40] F. Da Cunha Marinho,[2] C. L. Da Silva,[72] E. Dall'Occo,[43] J. Dalseno,[48] A. Davis,[3] O. De Aguiar Francisco,[40] K. De Bruyn,[40] S. De Capua,[56] M. De Cian,[12] J. M. De Miranda,[1] L. De Paula,[2] M. De Serio,[14,l] P. De Simone,[19] C. T. Dean,[53] D. Decamp,[4] L. Del Buono,[8] H.-P. Dembinski,[11] M. Demmer,[10] A. Dendek,[28] D. Derkach,[35] O. Deschamps,[5] F. Dettori,[54] B. Dey,[65] A. Di Canto,[40] P. Di Nezza,[19] H. Dijkstra,[40] F. Dordei,[40] M. Dorigo,[40] A. Dosil Suárez,[39] L. Douglas,[53] A. Dovbnya,[45] K. Dreimanis,[54] L. Dufour,[43] G. Dujany,[8] P. Durante,[40] J. M. Durham,[72] D. Dutta,[56] R. Dzhelyadin,[37] M. Dziewiecki,[12] A. Dziurda,[40] A. Dzyuba,[31] S. Easo,[51] M. Ebert,[52] U. Egede,[55] V. Egorychev,[32] S. Eidelman,[36,f] S. Eisenhardt,[52] U. Eitschberger,[10] R. Ekelhof,[10] L. Eklund,[53] S. Ely,[61] S. Esen,[12] H. M. Evans,[49] T. Evans,[57] A. Falabella,[15] N. Farley,[47] S. Farry,[54] D. Fazzini,[21,d] L. Federici,[25] D. Ferguson,[52] G. Fernandez,[38] P. Fernandez Declara,[40] A. Fernandez Prieto,[39] F. Ferrari,[15] L. Ferreira Lopes,[41] F. Ferreira Rodrigues,[2] M. Ferro-Luzzi,[40] S. Filippov,[34] R. A. Fini,[14] M. Fiorini,[17,a] M. Firlej,[28] C. Fitzpatrick,[41] T. Fiutowski,[28] F. Fleuret,[7,c] M. Fontana,[16,40] F. Fontanelli,[20,j] R. Forty,[40] V. Franco Lima,[54] M. Frank,[40] C. Frei,[40] J. Fu,[22,m] W. Funk,[40] E. Furfaro,[25,i] C. Färber,[40] E. Gabriel,[52] A. Gallas Torreira,[39] D. Galli,[15,h] S. Gallorini,[23] S. Gambetta,[52] M. Gandelman,[2] P. Gandini,[22] Y. Gao,[3] L. M. Garcia Martin,[70] J. García Pardiñas,[39] J. Garra Tico,[49] L. Garrido,[38] D. Gascon,[38] C. Gaspar,[40] L. Gavardi,[10] G. Gazzoni,[5] D. Gerick,[12] E. Gersabeck,[56] M. Gersabeck,[56] T. Gershon,[50] Ph. Ghez,[4] S. Gianì,[41] V. Gibson,[49] O. G. Girard,[41] L. Giubega,[30] K. Gizdov,[52] V. V. Gligorov,[8] D. Golubkov,[32] A. Golutvin,[55] A. Gomes,[1,n] I. V. Gorelov,[33] C. Gotti,[21,d] E. Govorkova,[43] J. P. Grabowski,[12] R. Graciani Diaz,[38] L. A. Granado Cardoso,[40] E. Graugés,[38] E. Graverini,[42] G. Graziani,[18] A. Grecu,[30] R. Greim,[9] P. Griffith,[16] L. Grillo,[56] L. Gruber,[40] B. R. Gruberg Cazon,[57] O. Grünberg,[67] E. Gushchin,[34] Yu. Guz,[37] T. Gys,[40] C. Göbel,[62] T. Hadavizadeh,[57] C. Hadjivasiliou,[5] G. Haefeli,[41] C. Haen,[40] S. C. Haines,[49] B. Hamilton,[60] X. Han,[12] T. H. Hancock,[57] S. Hansmann-Menzemer,[12] N. Harnew,[57] S. T. Harnew,[48] C. Hasse,[40] M. Hatch,[40] J. He,[63] M. Hecker,[55] K. Heinicke,[10] A. Heister,[9] K. Hennessy,[54] P. Henrard,[5] L. Henry,[70] E. van Herwijnen,[40] M. Heß,[67] A. Hicheur,[2] D. Hill,[57] P. H. Hopchev,[41] W. Hu,[65] W. Huang,[63] Z. C. Huard,[59] W. Hulsbergen,[43] T. Humair,[55] M. Hushchyn,[35] D. Hutchcroft,[54] P. Ibis,[10] M. Idzik,[28] P. Ilten,[47] R. Jacobsson,[40] J. Jalocha,[57] E. Jans,[43] A. Jawahery,[60] F. Jiang,[3] M. John,[57] D. Johnson,[40] C. R. Jones,[49] C. Joram,[40] B. Jost,[40] N. Jurik,[57] S. Kandybei,[45] M. Karacson,[40] J. M. Kariuki,[48] S. Karodia,[53] N. Kazeev,[35] M. Kecke,[12] F. Keizer,[49] M. Kelsey,[61] M. Kenzie,[49] T. Ketel,[44] E. Khairullin,[35] B. Khanji,[12] C. Khurewathanakul,[41] T. Kirn,[9] S. Klaver,[19] K. Klimaszewski,[29] T. Klimkovich,[11] S. Koliiev,[46] M. Kolpin,[12] I. Komarov,[41] R. Kopecna,[12] P. Koppenburg,[43] A. Kosmyntseva,[32] S. Kotriakhova,[31] M. Kozeiha,[5] L. Kravchuk,[34] M. Kreps,[50] F. Kress,[55] P. Krokovny,[36,f] W. Krzemien,[29] W. Kucewicz,[27,o] M. Kucharczyk,[27] V. Kudryavtsev,[36,f] A. K. Kuonen,[41] T. Kvaratskheliya,[32,40] D. Lacarrere,[40] G. Lafferty,[56] A. Lai,[16] G. Lanfranchi,[19] C. Langenbruch,[9] T. Latham,[50] C. Lazzeroni,[47] R. Le Gac,[6] A. Leflat,[33,40] J. Lefrançois,[7] R. Lefèvre,[5] F. Lemaitre,[40] E. Lemos Cid,[39] O. Leroy,[6] T. Lesiak,[27] B. Leverington,[12] P.-R. Li,[63] T. Li,[3] Y. Li,[7] Z. Li,[61] X. Liang,[61] T. Likhomanenko,[68] R. Lindner,[40] F. Lionetto,[42] V. Lisovskyi,[7] X. Liu,[3] D. Loh,[50] A. Loi,[16] I. Longstaff,[53] J. H. Lopes,[2] D. Lucchesi,[23,p] M. Lucio Martinez,[39] H. Luo,[52] A. Lupato,[23] E. Luppi,[17,a] O. Lupton,[40] A. Lusiani,[24] X. Lyu,[63] F. Machefert,[7] F. Maciuc,[30] V. Macko,[41] P. Mackowiak,[10] S. Maddrell-Mander,[48] O. Maev,[31,40] K. Maguire,[56] D. Maisuzenko,[31] M. W. Majewski,[28] S. Malde,[57] B. Malecki,[27] A. Malinin,[68] T. Maltsev,[36,f] G. Manca,[16,g] G. Mancinelli,[6] D. Marangotto,[22,m] J. Maratas,[5,q] J. F. Marchand,[4] U. Marconi,[15] C. Marin Benito,[38] M. Marinangeli,[41] P. Marino,[41] J. Marks,[12] G. Martellotti,[26] M. Martin,[6] M. Martinelli,[41] D. Martinez Santos,[39] F. Martinez Vidal,[70] A. Massafferri,[1] R. Matev,[40] A. Mathad,[50] Z. Mathe,[40] C. Matteuzzi,[21] A. Mauri,[42] E. Maurice,[7,c] B. Maurin,[41] A. Mazurov,[47] M. McCann,[55,40] A. McNab,[56] R. McNulty,[13] J. V. Mead,[54] B. Meadows,[59] C. Meaux,[6] F. Meier,[10] N. Meinert,[67] D. Melnychuk,[29] M. Merk,[43] A. Merli,[22,40,m] E. Michielin,[23] D. A. Milanes,[66] E. Millard,[50] M.-N. Minard,[4] L. Minzoni,[17] D. S. Mitzel,[12] A. Mogini,[8] J. Molina Rodriguez,[1] T. Mombächer,[10] I. A. Monroy,[66] S. Monteil,[5] M. Morandin,[23] M. J. Morello,[24,k] O. Morgunova,[68] J. Moron,[28] A. B. Morris,[52] R. Mountain,[61] F. Muheim,[52] M. Mulder,[43] D. Müller,[56] J. Müller,[10] K. Müller,[42] V. Müller,[10] P. Naik,[48] T. Nakada,[41] R. Nandakumar,[51] A. Nandi,[57] I. Nasteva,[2] M. Needham,[52] N. Neri,[22,40] S. Neubert,[12] N. Neufeld,[40] M. Neuner,[12] T. D. Nguyen,[41] C. Nguyen-Mau,[41,r] S. Nieswand,[9] R. Niet,[10] N. Nikitin,[33] T. Nikodem,[12] A. Nogay,[68] D. P. O'Hanlon,[50] A. Oblakowska-Mucha,[28] V. Obraztsov,[37] S. Ogilvy,[19] R. Oldeman,[16,g] C. J. G. Onderwater,[71] A. Ossowska,[27] J. M. Otalora Goicochea,[2] P. Owen,[42] A. Oyanguren,[70] P. R. Pais,[41] A. Palano,[14] M. Palutan,[19,40] A. Papanestis,[51] M. Pappagallo,[52] L. L. Pappalardo,[17,a] W. Parker,[60] C. Parkes,[56] G. Passaleva,[18,40] A. Pastore,[14,l] M. Patel,[55] C. Patrignani,[15,h] A. Pearce,[40] A. Pellegrino,[43] G. Penso,[26] M. Pepe Altarelli,[40] S. Perazzini,[40] D. Pereima,[32] P. Perret,[5] L. Pescatore,[41] K. Petridis,[48] A. Petrolini,[20,j] A. Petrov,[68] M. Petruzzo,[22,m] E. Picatoste Olloqui,[38] B. Pietrzyk,[4] G. Pietrzyk,[41] M. Pikies,[27] D. Pinci,[26] F. Pisani,[40] A. Pistone,[20,j] A. Piucci,[12]

V. Placinta,[30] S. Playfer,[52] M. Plo Casasus,[39] F. Polci,[8] M. Poli Lener,[19] A. Poluektov,[50] I. Polyakov,[61] E. Polycarpo,[2] G. J. Pomery,[48] S. Ponce,[40] A. Popov,[37] D. Popov,[11,40] S. Poslavskii,[37] C. Potterat,[2] E. Price,[48] J. Prisciandaro,[39] C. Prouve,[48] V. Pugatch,[46] A. Puig Navarro,[42] H. Pullen,[57] G. Punzi,[24,s] W. Qian,[50] J. Qin,[63] R. Quagliani,[8] B. Quintana,[5] B. Rachwal,[28] J. H. Rademacker,[48] M. Rama,[24] M. Ramos Pernas,[39] M. S. Rangel,[2] I. Raniuk,[45†] F. Ratnikov,[35] G. Raven,[44] M. Ravonel Salzgeber,[40] M. Reboud,[4] F. Redi,[41] S. Reichert,[10] A. C. dos Reis,[1] C. Remon Alepuz,[70] V. Renaudin,[7] S. Ricciardi,[51] S. Richards,[48] M. Rihl,[40] K. Rinnert,[54] P. Robbe,[7] A. Robert,[8] A. B. Rodrigues,[41] E. Rodrigues,[59] J. A. Rodriguez Lopez,[66] A. Rogozhnikov,[35] S. Roiser,[40] A. Rollings,[57] V. Romanovskiy,[37] A. Romero Vidal,[39,40] M. Rotondo,[19] M. S. Rudolph,[61] T. Ruf,[40] P. Ruiz Valls,[70] J. Ruiz Vidal,[70] J. J. Saborido Silva,[39] E. Sadykhov,[32] N. Sagidova,[31] B. Saitta,[16,g] V. Salustino Guimaraes,[62] C. Sanchez Mayordomo,[70] B. Sanmartin Sedes,[39] R. Santacesaria,[26] C. Santamarina Rios,[39] M. Santimaria,[19] E. Santovetti,[25,i] G. Sarpis,[56] A. Sarti,[19,t] C. Satriano,[26,u] A. Satta,[25] D. M. Saunders,[48] D. Savrina,[32,33] S. Schael,[9] M. Schellenberg,[10] M. Schiller,[53] H. Schindler,[40] M. Schmelling,[11] T. Schmelzer,[10] B. Schmidt,[40] O. Schneider,[41] A. Schopper,[40] H. F. Schreiner,[59] M. Schubiger,[41] M. H. Schune,[7] R. Schwemmer,[40] B. Sciascia,[19] A. Sciubba,[26,t] A. Semennikov,[32] E. S. Sepulveda,[8] A. Sergi,[47] N. Serra,[42] J. Serrano,[6] L. Sestini,[23] P. Seyfert,[40] M. Shapkin,[37] I. Shapoval,[45] Y. Shcheglov,[31] T. Shears,[54] L. Shekhtman,[36,f] V. Shevchenko,[68] B. G. Siddi,[17] R. Silva Coutinho,[42] L. Silva de Oliveira,[2] G. Simi,[23,p] S. Simone,[14,l] M. Sirendi,[49] N. Skidmore,[48] T. Skwarnicki,[61] I. T. Smith,[52] J. Smith,[49] M. Smith,[55] l. Soares Lavra,[1] M. D. Sokoloff,[59] F. J. P. Soler,[53] B. Souza De Paula,[2] B. Spaan,[10] P. Spradlin,[53] S. Sridharan,[40] F. Stagni,[40] M. Stahl,[12] S. Stahl,[40] P. Stefko,[41] S. Stefkova,[55] O. Steinkamp,[42] S. Stemmle,[12] O. Stenyakin,[37] M. Stepanova,[31] H. Stevens,[10] S. Stone,[61] B. Storaci,[42] S. Stracka,[24,s] M. E. Stramaglia,[41] M. Straticiuc,[30] U. Straumann,[42] J. Sun,[3] L. Sun,[64] K. Swientek,[28] V. Syropoulos,[44] T. Szumlak,[28] M. Szymanski,[63] S. T'Jampens,[4] A. Tayduganov,[6] T. Tekampe,[10] G. Tellarini,[17,a] F. Teubert,[40] E. Thomas,[40] J. van Tilburg,[43] M. J. Tilley,[55] V. Tisserand,[5] M. Tobin,[41] S. Tolk,[49] L. Tomassetti,[17,a] D. Tonelli,[24] R. Tourinho Jadallah Aoude,[1] E. Tournefier,[4] M. Traill,[53] M. T. Tran,[41] M. Tresch,[42] A. Trisovic,[49] A. Tsaregorodtsev,[6] P. Tsopelas,[43] A. Tully,[49] N. Tuning,[43,40] A. Ukleja,[29] A. Usachov,[7] A. Ustyuzhanin,[35] U. Uwer,[12] C. Vacca,[16,g] A. Vagner,[69] V. Vagnoni,[15,40] A. Valassi,[40] S. Valat,[40] G. Valenti,[15] R. Vazquez Gomez,[40] P. Vazquez Regueiro,[39] S. Vecchi,[17] M. van Veghel,[43] J. J. Velthuis,[48] M. Veltri,[18,v] G. Veneziano,[57] A. Venkateswaran,[61] T. A. Verlage,[9] M. Vernet,[5] M. Veronesi,[43] M. Vesterinen,[57] J. V. Viana Barbosa,[40] D. Vieira,[63] M. Vieites Diaz,[39] H. Viemann,[67] X. Vilasis-Cardona,[38,b] M. Vitti,[49] V. Volkov,[33] A. Vollhardt,[42] B. Voneki,[40] A. Vorobyev,[31] V. Vorobyev,[36,f] C. Voß,[9] J. A. de Vries,[43] C. Vázquez Sierra,[43] R. Waldi,[67] J. Walsh,[24] J. Wang,[61] Y. Wang,[65] D. R. Ward,[49] H. M. Wark,[54] N. K. Watson,[47] D. Websdale,[55] A. Weiden,[42] C. Weisser,[58] M. Whitehead,[40] J. Wicht,[50] G. Wilkinson,[57] M. Wilkinson,[61] M. Williams,[56] M. Williams,[58] T. Williams,[47] F. F. Wilson,[51,40] J. Wimberley,[60] M. Winn,[7] J. Wishahi,[10] W. Wislicki,[29] M. Witek,[27] G. Wormser,[7] S. A. Wotton,[49] K. Wyllie,[40] Y. Xie,[65] M. Xu,[65] Q. Xu,[63] Z. Xu,[3] Z. Xu,[4] Z. Yang,[3] Z. Yang,[60] Y. Yao,[61] H. Yin,[65] J. Yu,[65] X. Yuan,[61] O. Yushchenko,[37] K. A. Zarebski,[47] M. Zavertyaev,[11,w] L. Zhang,[3] Y. Zhang,[7] A. Zhelezov,[12] Y. Zheng,[63] X. Zhu,[3] V. Zhukov,[9,33] J. B. Zonneveld,[52] and S. Zucchelli[15]

(LHCb Collaboration)

[1]*Centro Brasileiro de Pesquisas Físicas (CBPF), Rio de Janeiro, Brazil*
[2]*Universidade Federal do Rio de Janeiro (UFRJ), Rio de Janeiro, Brazil*
[3]*Center for High Energy Physics, Tsinghua University, Beijing, China*
[4]*Univ. Grenoble Alpes, Univ. Savoie Mont Blanc, CNRS, IN2P3-LAPP, Annecy, France*
[5]*Clermont Université, Université Blaise Pascal, CNRS/IN2P3, LPC, Clermont-Ferrand, France*
[6]*Aix Marseille Univ, CNRS/IN2P3, CPPM, Marseille, France*
[7]*LAL, Univ. Paris-Sud, CNRS/IN2P3, Université Paris-Saclay, Orsay, France*
[8]*LPNHE, Université Pierre et Marie Curie, Université Paris Diderot, CNRS/IN2P3, Paris, France*
[9]*I. Physikalisches Institut, RWTH Aachen University, Aachen, Germany*
[10]*Fakultät Physik, Technische Universität Dortmund, Dortmund, Germany*
[11]*Max-Planck-Institut für Kernphysik (MPIK), Heidelberg, Germany*
[12]*Physikalisches Institut, Ruprecht-Karls-Universität Heidelberg, Heidelberg, Germany*
[13]*School of Physics, University College Dublin, Dublin, Ireland*
[14]*Sezione INFN di Bari, Bari, Italy*
[15]*Sezione INFN di Bologna, Bologna, Italy*
[16]*Sezione INFN di Cagliari, Cagliari, Italy*
[17]*Universita e INFN, Ferrara, Ferrara, Italy*

[18]*Sezione INFN di Firenze, Firenze, Italy*
[19]*Laboratori Nazionali dell'INFN di Frascati, Frascati, Italy*
[20]*Sezione INFN di Genova, Genova, Italy*
[21]*Sezione INFN di Milano Bicocca, Milano, Italy*
[22]*Sezione di Milano, Milano, Italy*
[23]*Sezione INFN di Padova, Padova, Italy*
[24]*Sezione INFN di Pisa, Pisa, Italy*
[25]*Sezione INFN di Roma Tor Vergata, Roma, Italy*
[26]*Sezione INFN di Roma La Sapienza, Roma, Italy*
[27]*Henryk Niewodniczanski Institute of Nuclear Physics Polish Academy of Sciences, Kraków, Poland*
[28]*AGH - University of Science and Technology, Faculty of Physics and Applied Computer Science, Kraków, Poland*
[29]*National Center for Nuclear Research (NCBJ), Warsaw, Poland*
[30]*Horia Hulubei National Institute of Physics and Nuclear Engineering, Bucharest-Magurele, Romania*
[31]*Petersburg Nuclear Physics Institute (PNPI), Gatchina, Russia*
[32]*Institute of Theoretical and Experimental Physics (ITEP), Moscow, Russia*
[33]*Institute of Nuclear Physics, Moscow State University (SINP MSU), Moscow, Russia*
[34]*Institute for Nuclear Research of the Russian Academy of Sciences (INR RAN), Moscow, Russia*
[35]*Yandex School of Data Analysis, Moscow, Russia*
[36]*Budker Institute of Nuclear Physics (SB RAS), Novosibirsk, Russia*
[37]*Institute for High Energy Physics (IHEP), Protvino, Russia*
[38]*ICCUB, Universitat de Barcelona, Barcelona, Spain*
[39]*Instituto Galego de Física de Altas Enerxías (IGFAE), Universidade de Santiago de Compostela, Santiago de Compostela, Spain*
[40]*European Organization for Nuclear Research (CERN), Geneva, Switzerland*
[41]*Institute of Physics, Ecole Polytechnique Fédérale de Lausanne (EPFL), Lausanne, Switzerland*
[42]*Physik-Institut, Universität Zürich, Zürich, Switzerland*
[43]*Nikhef National Institute for Subatomic Physics, Amsterdam, The Netherlands*
[44]*Nikhef National Institute for Subatomic Physics and VU University Amsterdam, Amsterdam, The Netherlands*
[45]*NSC Kharkiv Institute of Physics and Technology (NSC KIPT), Kharkiv, Ukraine*
[46]*Institute for Nuclear Research of the National Academy of Sciences (KINR), Kyiv, Ukraine*
[47]*University of Birmingham, Birmingham, United Kingdom*
[48]*H.H. Wills Physics Laboratory, University of Bristol, Bristol, United Kingdom*
[49]*Cavendish Laboratory, University of Cambridge, Cambridge, United Kingdom*
[50]*Department of Physics, University of Warwick, Coventry, United Kingdom*
[51]*STFC Rutherford Appleton Laboratory, Didcot, United Kingdom*
[52]*School of Physics and Astronomy, University of Edinburgh, Edinburgh, United Kingdom*
[53]*School of Physics and Astronomy, University of Glasgow, Glasgow, United Kingdom*
[54]*Oliver Lodge Laboratory, University of Liverpool, Liverpool, United Kingdom*
[55]*Imperial College London, London, United Kingdom*
[56]*School of Physics and Astronomy, University of Manchester, Manchester, United Kingdom*
[57]*Department of Physics, University of Oxford, Oxford, United Kingdom*
[58]*Massachusetts Institute of Technology, Cambridge, MA, United States*
[59]*University of Cincinnati, Cincinnati, OH, United States*
[60]*University of Maryland, College Park, MD, United States*
[61]*Syracuse University, Syracuse, NY, United States*
[62]*Pontifícia Universidade Católica do Rio de Janeiro (PUC-Rio), Rio de Janeiro, Brazil (associated with Institution Universidade Federal do Rio de Janeiro (UFRJ), Rio de Janeiro, Brazil)*
[63]*University of Chinese Academy of Sciences, Beijing, China (associated with Institution Center for High Energy Physics, Tsinghua University, Beijing, China)*
[64]*School of Physics and Technology, Wuhan University, Wuhan, China (associated with Institution Center for High Energy Physics, Tsinghua University, Beijing, China)*
[65]*Institute of Particle Physics, Central China Normal University, Wuhan, Hubei, China (associated with Institution Center for High Energy Physics, Tsinghua University, Beijing, China)*
[66]*Departamento de Fisica, Universidad Nacional de Colombia, Bogota, Colombia (associated with Institution LPNHE, Université Pierre et Marie Curie, Université Paris Diderot, CNRS/IN2P3, Paris, France)*

[67]*Institut für Physik, Universität Rostock, Rostock, Germany*
(associated with Institution Physikalisches Institut, Ruprecht-Karls-Universität Heidelberg, Heidelberg, Germany)
[68]*National Research Centre Kurchatov Institute, Moscow, Russia*
(associated with Institution Institute of Theoretical and Experimental Physics (ITEP), Moscow, Russia)
[69]*National Research Tomsk Polytechnic University, Tomsk, Russia*
(associated with Institution Institute of Theoretical and Experimental Physics (ITEP), Moscow, Russia)
[70]*Instituto de Fisica Corpuscular, Centro Mixto Universidad de Valencia - CSIC, Valencia, Spain*
(associated with Institution ICCUB, Universitat de Barcelona, Barcelona, Spain)
[71]*Van Swinderen Institute, University of Groningen, Groningen, The Netherlands*
(associated with Institution Nikhef National Institute for Subatomic Physics, Amsterdam, The Netherlands)
[72]*Los Alamos National Laboratory (LANL), Los Alamos, United States*
(associated with Institution Syracuse University, Syracuse, NY, United States)

[†]Deceased.
[a]Also at Università di Ferrara, Ferrara, Italy.
[b]Also at LIFAELS, La Salle, Universitat Ramon Llull, Barcelona, Spain.
[c]Also at Laboratoire Leprince-Ringuet, Palaiseau, France.
[d]Also at Università di Milano Bicocca, Milano, Italy.
[e]Also at Università di Modena e Reggio Emilia, Modena, Italy.
[f]Also at Novosibirsk State University, Novosibirsk, Russia.
[g]Also at Università di Cagliari, Cagliari, Italy.
[h]Also at Università di Bologna, Bologna, Italy.
[i]Also at Università di Roma Tor Vergata, Roma, Italy.
[j]Also at Università di Genova, Genova, Italy.
[k]Also at Scuola Normale Superiore, Pisa, Italy.
[l]Also at Università di Bari, Bari, Italy.
[m]Also at Università degli Studi di Milano, Milano, Italy.
[n]Also at Universidade Federal do Triângulo Mineiro (UFTM), Uberaba-MG, Brazil.
[o]Also at AGH - University of Science and Technology, Faculty of Computer Science, Electronics and Telecommunications, Kraków, Poland.
[p]Also at Università di Padova, Padova, Italy.
[q]Also at Iligan Institute of Technology (IIT), Iligan, Philippines.
[r]Also at Hanoi University of Science, Hanoi, Vietnam.
[s]Also at Università di Pisa, Pisa, Italy.
[t]Also at Università di Roma La Sapienza, Roma, Italy.
[u]Also at Università della Basilicata, Potenza, Italy.
[v]Also at Università di Urbino, Urbino, Italy.
[w]Also at P.N. Lebedev Physical Institute, Russian Academy of Science (LPI RAS), Moscow, Russia.